Sonic logging in deviated wellbores in the presence of a drill collar

Bikash K. Sinha, Schlumberger-Doll Research, and Ergun Simsek, Bahcesehir University*

Summary

Acquiring sonic logs while drilling is far more challenging than acquiring sonic logs from a wireline tool, notably because of the higher noise level in the drilling environment. The presence of a drill collar in the form of a thick steel pipe motivates a different tool design strategy. In addition, interference of drilling noise with the formation signal requires new processing and inversion algorithms for estimating the formation compressional and shear slownesses. Generally, all wireline sonic tools estimate the formation shear slowness by processing the borehole flexural arrival that is not severely affected by the tool structure. However, to mitigate interference between the drill collar and formation arrivals in the LWD (Logging-While-Drilling) environment, there has been a growing interest in inverting the borehole quadrupole dispersive arrival for the formation shear slowness. Inversion of quadrupole dispersion yields the same formation shear as that from a dipole shear logging tool in an isotropic and transversely-isotropic (TI) formation when the borehole axis is parallel to the TI-symmetry axis. Nevertheless, it is known that in anisotropic formations, we can have three different shear moduli in the three orthogonal planes. It is then necessary to understand which of the three shear moduli or some combination thereof, would be estimated from the inversion of quadrupole sonic data from a LWD tool in deviated boreholes in TI formations.

A finite-difference time domain (FDTD) formulation with a perfectly-matched layer (PML) enables analysis of elastic wave propagation in a fluid-filled borehole in an arbitrarily anisotropic formation in the presence of a drill collar. Introduction of a perfectly-matched boundary layer minimizes reflections from the boundary with a limited grid volume. The FDTD formulation yields synthetic waveforms at an array of receivers produced by a monopole, dipole or quadrupole source placed on the borehole axis. Synthetic waveforms are then processed by a modified matrix pencil algorithm to isolate both non-dispersive and dispersive arrivals in the wavetrain. Computational results have been obtained for various modal arrivals generated by either a monopole, dipole, or quadrupole source placed in a fluid-filled borehole. While dipole flexural dispersions provide estimates of shear rigidity in the two orthogonal borehole axial planes, the monopole Stoneley dispersion can be inverted to estimate the shear rigidity in the borehole cross-sectional plane. In contrast, quadrupole waves simultaneously vibrate the formation in the two orthogonal axial planes. Therefore, inversion of low-frequency quadrupole dispersion based on an isotropic model yields a shear modulus that is some combination of the fast and slow shear moduli in the two orthogonal axial planes.

Introduction

Recent focus on shale gas production has renewed interest in a complete anisotropy characterization of shale reservoirs. Shale gas production is faced with a new challenge of understanding formation anisotropy and subsequent analysis to identify the source of observed anisotropy. Formation anisotropy plays an important role in the design of hydraulic fracturing operation for enhancing shale-gas production. To increase the producing well contact with a reservoir, most of such wells are horizontally drilled in a TI-shale. Cross-dipole data in such horizontal wells would, in principle, yield the formation shear moduli in the two orthogonal borehole axial planes. These two shear moduli provide an estimate of the Thomsen parameter γ for a TI shale formation (Thomsen, 1986).

This paper describes results from a FDTD formulation of elastic wave propagation in a fluid-filled borehole in formations exhibiting triclinic symmetry with 21 independent elastic moduli. Synthetic waveforms generated by a monopole, dipole, and quadrupole sources have been processed to estimate the compressional slowness along the borehole axis; and the Stoneley and dipole shear slownesses in the borehole cross-sectional and axial planes, respectively. The zero-frequency intercept of the Stoneley dispersion yields the tube wave velocity, whereas low-frequency asymptotes of the fast and slow dipole dispersions correspond to the SH- and qSV-polarized shear wave velocities. In particular, this study promotes understanding of what quadrupole shear logging provides in these horizontal wells in a TI-formation in the presence of a drill collar.

Theory

A horizontally layered structure exhibits transversely-isotropic (TI) anisotropy with a vertical (X_3-) axis of symmetry. A TI-anisotropy is also referred to as polar anisotropy with 5 independent anisotropic moduli. Figure 1 shows a schematic diagram of a vertical well parallel to the X_3-axis, and a deviated well with azimuth ϕ and deviation θ. The well deviation is defined by rotating the TI-anisotropy axes by angle θ about the X_1-axis in the isotropic plane.

When the propagation direction is parallel to the TI-symmetry axis, there is one longitudinal wave, and there are two degenerate transverse waves that propagate with the same velocity. In contrast, when the propagation direction is perpendicular to the TI-symmetry axis, there is one longitudinal wave, and two distinct, mutually orthogonal, pure transverse waves with different velocities. However, when the propagation direction is obliquely inclined to the TI-symmetry axis, as is the case in a deviated wellbore, the anisotropic medium supports a

purely transverse (SH) mode, and two mixed (qP and qSV) modes of plane waves (Norris and Sinha, 1993).

Analytical solutions of elastic waves in a fluid-filled borehole can be obtained only in a TI-formation with its symmetry axis (TIV) parallel to the borehole axis (White and Tongtaow, 1981; Chan and Tsang, 1983; Ellefsen et al., 1991). Most of the anisotropic environments including a TI-formation with horizontal axis of symmetry (TIH) require the use of a perturbation technique or a numerical FDTD formulation of the linear equations of motion in anisotropic materials. Sinha et al., (1994) proposed the use of an equivalent isotropic reference state in a perturbation model to account for an arbitrary state of formation anisotropy. It has been also demonstrated that a properly selected equivalent isotropic state adequately accounts for most of the weakly anisotropic formations (Thomsen, 1986). This choice of an equivalent isotropic reference state minimizes the amount of perturbative correction in the modal dispersions to account for the remaining formation structural anisotropy.

We analyze wave propagation in deviated wellbores using a finite-difference formulation of equations of motion in 3D-cylindrical coordinates applied to a fluid-filled borehole in an arbitrarily anisotropic formation (Liu and Sinha, 2003). This formulation accounts for the presence of a drill collar in the form of a thick steel pipe.

Computational Results

As an illustrative example, we describe computational results for the plane wave and borehole modal slownesses in deviated wellbores in a fast TI-formation (Bakken shale). Results for the plane wave slownesses and associated polarization vectors are obtained from the solution of Kelvin-Christoffel equations for an arbitrary propagation direction from the TI-symmetry axis. The elastic constants and mass density of Bakken shale are given in Sinha et al., (1994). The shear slowness of a fast formation is smaller than the borehole liquid compressional slowness. Since a TI-material is invariant with respect to any rotation about its symmetry axis (or equivalently, the well azimuth in a formation with a vertical TI-symmetry axis), we show in Figure 2, the qSV-shear and SH-shear wave slownesses as a function of well deviation θ from the TI-symmetry axis. Similar calculations for the tube wave and compressional wave slownesses show that the tube wave velocity changes by only about 3% over the entire range of wellbore deviations, whereas the shear and compressional wave slownesses change by up to about 12 to 25%, respectively.

Drill collar effects on borehole modes: TIV Bakken shale

When a wellbore is parallel to the TI-symmetry axis, the wellbore cross-sectional plane exhibits isotropy implying that all axial planes would have the same shear rigidity. Consequently, cross-dipole slownesses do not show any azimuthal anisotropy. However, shear rigidities in the borehole axial and cross-sectional planes are different and can be expressed in terms of the Thomsen gamma parameter. Computational results have been obtained for a drill collar with inner and outer radii of 6 and 8.5 cm, respectively. The collar is concentrically placed in a water-filled borehole of radius 12 cm. A ring source is placed at a radius of 11.5 cm, and is 90 cm from the first receiver. The inter-receiver spacing is 8 cm. Synthetic waveforms have been generated by a 3D-cylindrical FDTD method and processed by a modified matrix pencil algorithm to isolate both dispersive and non-dispersive arrivals in the wavetrain (Ekstrom, 1995). The left subplot in Figure 3 shows an array of synthetic waveforms produced by a monopole source in the absence (blue) and presence (red) of a drill collar. The right subplot in Figure 3 displays the corresponding Stoneley dispersions with and without the drill collar by the blue and red curves, respectively. Notice that the presence of a drill collar causes the Stoneley dispersion to become slower than that in the absence of any tool structure at all frequencies. The zero-frequency intercept of the Stoneley dispersion is also consistent with the analytical result for the tube wave slowness for this configuration.

We show in the left subplot in Figure 4 an array of synthetic waveforms produced by a dipole source in the absence (red) and presence (blue) of a drill collar. The right subplot in Figure 4 depicts the corresponding flexural dispersions with and without the drill collar by the blue and red curves, respectively. The slowest modal dispersion (shown by the upper blue curve) in the presence of a drill collar is dominated by the pipe flexural mode at low frequencies. In contrast, the high-frequency part of the dispersion is sensitive to both the borehole fluid and formation parameters. However, the formation flexural dispersion (shown by the lower blue curve) asymptotes to the formation shear slowness at low frequencies for such fast TI formations. Interestingly, this flexural dispersion is significantly faster at higher frequencies than the dispersion obtained in the absence of any drill collar as denoted by the red curve.

The left subplot in Figure 5 shows arrays of synthetic waveforms produced by a quadrupole source in the absence (red) and presence (blue) of a drill collar. The right subplot in Figure 5 displays the corresponding quadrupole dispersions without and with the drill collar by the red and blue curves, respectively. As is the case with the dipole flexural dispersion, the presence of a drill collar structure causes a significant flattening of the quadrupole dispersion at higher frequencies. Interestingly, the drill collar (or pipe) quadrupole mode remains far away from the formation quadrupole dispersion.

Horizontal wellbore in a TI formation: TIH Bakken shale

When a wellbore is perpendicular to the TI-symmetry (X_3-) axis, differences between the two cross-dipole shear slownesses are related to the Thomsen gamma parameter. The left subplot in Figure 6 compares arrays of synthetic waveforms generated by a quadrupole source placed in a TIV (blue) and TIH (red) Bakken shale formations. The right subplot in Figure 6 displays the corresponding quadrupole dispersions for the TIV (red) and TIH (blue) formations, respectively.

Wellbore deviation 60 degrees in a TI Bakken shale

The left subplot in Figure 7 depicts arrays of quadrupole waveforms obtained in a TIV (blue) Bakken shale and in a 60^o deviated wellbore (red) in the presence of a drill collar. The right subplot in Figure 7 compares the corresponding quadrupole dispersions obtained from the synthetic waveforms in a TIV formation with that obtained in a 60 degrees deviated wellbore. Notice that the low-frequency quadrupole shear approaches the degenerate SH and qSV slownesses, which are identically the same in a TIV formation. However, low-frequency quadrupole dispersion approaches shear slownesses that are between the SH and qSV wave shear slownesses for a 60 degrees propagation from the TI-symmetry axis.

Horizontal wellbore in a TI formation: TIH Austin chalk

Next we compare dipole flexural and quadrupole waves propagating along a wellbore perpendicular to the TI-symmetry axis in a slow Austin chalk formation. The left subplot in Figure 8 shows arrays of synthetic waveforms produced by a dipole (red) and quadrupole (blue) transmitters. Processing of these waveforms yields the corresponding formation and pipe flexural modes (in red), and the formation quadrupole dispersion (in blue) as shown in the right subplot in Figure 8. As is the case for a deviated wellbore in a TI formation, we observe that the low-frequency quadrupole dispersion approaches the SH and qSV wave slownesses for a 90 degrees propagation from the TI-symmetry axis.

Summary and Conclusions

We have used a 3D cylindrical FDTD with PML formulation of the linear equations of motion in arbitrarily anisotropic materials to study influence of a drill collar (or a steel pipe) structure on elastic wave propagation in a fluid-filled borehole in both a TI- and tilted TI-formations. A tilted TI-formation refers to a wellbore with dipping beds or a deviated wellbore with its axis obliquely inclined with respect to the TI-symmetry axis.

Computational results for the Stoneley dispersion show negligibly small changes consistent with small changes in the tube wave velocity for different wellbore deviations. The tube wave velocity obtained from the zero-frequency intercept of the Stoneley dispersion in the absence of any tool structure compares very well with the analytical results for a range of well deviations in both fast and slow transversely-isotropic (TI) formations.

In contrast, cross-dipole dispersions exhibit relatively larger differences consistent with the qSV- and SH- wave slownesses as a function of wellbore deviation from the TI-symmetry axis. Good agreement is also obtained between low-frequency asymptotes of borehole flexural dispersions and the corresponding shear wave velocities from a numerically exact solution of Kelvin-Christoffel equations for plane wave velocities in an arbitrarily anisotropic formation.

More importantly, we observe that the quadrupole dispersion at low frequencies approaches a shear slowness in between the fast and slow shear slownesses in the two orthogonal axial planes. This is consistent with the observation that quadrupole waves vibrate the formation in the two orthogonal planes, and therefore, would be sensitive to shear rigidities in those two axial planes.

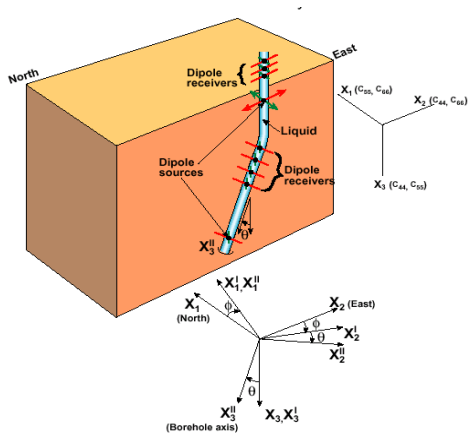

Figure 1: Schematic diagram of a vertical well parallel to the X_3-axis and a deviated well with azimuth ϕ and deviation θ.

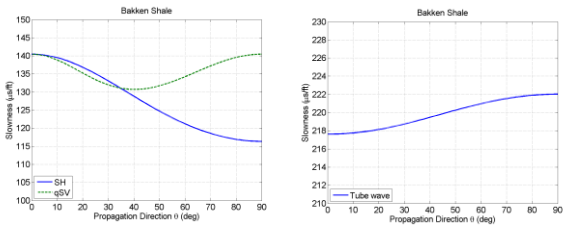

Figure 2: qSV- and SH-wave phase slownesses (left subplot) and tube wave slowness (right subplot) as a function of propagation direction from the TI-symmetry axis in a fast Bakken shale formation.

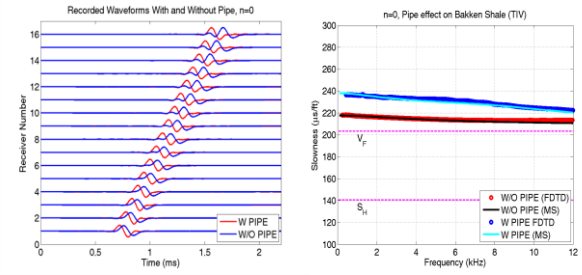

Figure 3: Synthetic monopole waves (left subplot) and corresponding Stoneley dispersions (right subplot) in the absence (red) and presence (blue) of a drill collar in a TI Bakken shale formation with the borehole parallel ($\theta=0^o$) to the TI-symmetry axis.

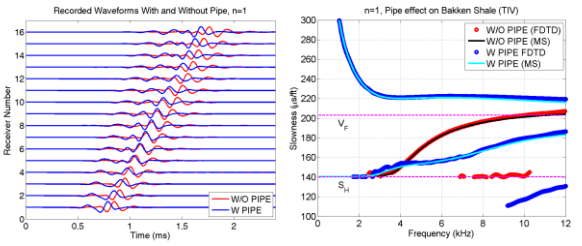

Figure 4: Synthetic dipole waves (left subplot) and corresponding borehole flexural dispersions (right subplot) in the absence (red) and presence (blue) of a drill collar in a TI Bakken shale formation with the borehole parallel ($\theta=0^o$) to the TI-symmetry axis. Curves labeled MS and FDTD, respectively, denote dispersion results from a root-finding mode-search routine and those obtained from the processing of synthetic waveforms.

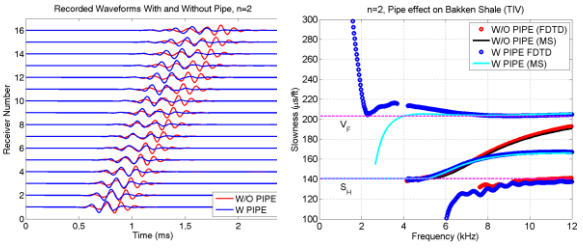

Figure 5: Synthetic quadrupole waves (left subplot) and corresponding borehole quadrupole dispersions (right subplot) in the absence (red) and presence (blue) of a drill collar in a TI Bakken shale formation with the borehole parallel ($\theta=0^o$) to the TI-symmetry axis.

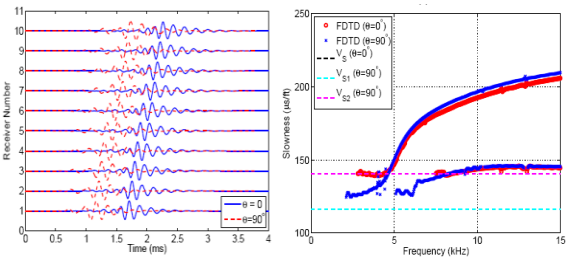

Figure 6: Synthetic quadrupole waves (left subplot) and corresponding borehole quadrupole dispersions (right subplot) in the presence of a drill collar in a TI Bakken shale formation with the borehole parallel ($\theta=0^o$, shown in red) and perpendicular ($\theta=90^o$, shown in blue) to the TI-symmetry axis.

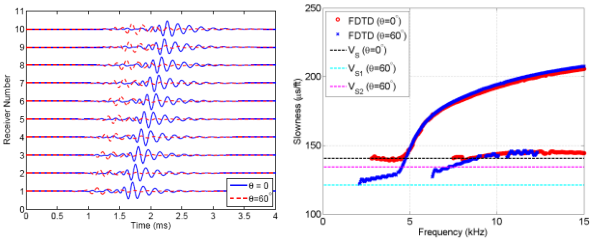

Figure 7: Synthetic quadrupole waves (left subplot) and corresponding borehole quadrupole dispersions (right subplot) in the presence of a drill collar in a TI Bakken shale formation with the borehole parallel ($\theta=0^o$, shown in red) and perpendicular ($\theta=60^o$, shown in blue) to the TI-symmetry axis.

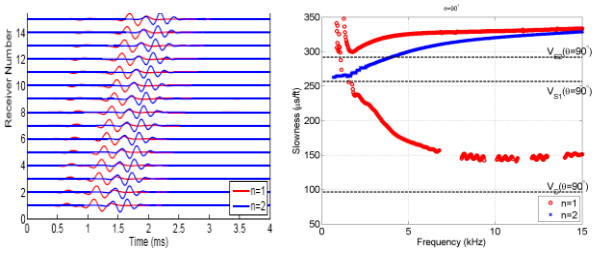

Figure 8: Synthetic dipole flexural (n=1) and quadrupole (n=2) waves (left subplot) and corresponding borehole dipole and quadrupole dispersions (right subplot) in the presence of a drill collar in a TI Austin chalk formation with the borehole perpendicular ($\theta=90^o$) to the TI-symmetry axis. The red and blue curves, respectively, denote the dipole flexural and quadrupole dispersions.

EDITED REFERENCES

Note: This reference list is a copy-edited version of the reference list submitted by the author. Reference lists for the 2010 SEG Technical Program Expanded Abstracts have been copy edited so that references provided with the online metadata for each paper will achieve a high degree of linking to cited sources that appear on the Web.

REFERENCES

Chan, A. K., and T. Tsang, 1983, Propagation of acoustic waves in a fluid-filled borehole surrounded by a concentrically layered transversely isotropic formation: The Journal of the Acoustical Society of America, **74**, no. 5, 1605–1616, doi:10.1121/1.390122.

Ekstrom, M. E., 1995, Dispersion estimation from borehole acoustic arrays using a modified matrix pencil algorithm: Presented at the 29th Asilomar Conference on Signals, Systems, and Computers, Pacific Grove, California, October 31.

Ellefsen, K. J., C. H. Cheng, and M. N. Toksoz, 1991, Effects of anisotropy upon the normal modes in a borehole: The Journal of the Acoustical Society of America, **89**, no. 6, 2597–2616, doi:10.1121/1.400699.

Liu, Q. H., and B. K. Sinha, 2003, A 3D cylindrical PML/FDTD method for elastic waves in fluid-filled pressurized boreholes in triaxially stressed formations: Geophysics, **68**, 1731–1743, doi:10.1190/1.1620646.

Norris, A. N., and B. K. Sinha, 1993, Weak elastic anisotropy and the tube wave: Geophysics, **58**, 1091, doi:10.1190/1.1443493.

Sinha, B. K., A. N. Norris, and S. K. Chang, 1994, Borehole flexural modes in anisotropic formations: Geophysics, **59**, 1037–1052, doi:10.1190/1.1443660.

Thomsen, L., 1986, Weak elastic anisotropy: Geophysics, **51**, 1954–1966, doi:10.1190/1.1442051.

White, J. E., and C. Tongtaow, 1981, Cylindrical waves in transversely isotropic media: The Journal of the Acoustical Society of America, **70**, no. 4, 1147–1155, doi:10.1121/1.386946.